May 2002 • NREL/CP-520-32283

Conference Paper

In-situ Characterization of the Amorphous to Microcrystalline Transition in Hot-Wire CVD Growth of Si:H Using Real Time Spectroscopic Ellipsometry

Preprint

D.H. Levi, B.P. Nelson, J.D. Perkins, and H.R. Moutinho

To be presented at the 29th IEEE PV Specialists Conference
New Orleans, Louisiana
May 20-24, 2002

National Renewable Energy Laboratory

1617 Cole Boulevard
Golden, Colorado 80401-3393

NREL is a U.S. Department of Energy Laboratory
Operated by Midwest Research Institute • Battelle • Bechtel

Contract No. DE-AC36-99-GO10337

IN-SITU CHARACTERIZATION OF THE AMORPHOUS TO MICROSCRYSTALLINE TRANSITION IN HOT WIRE CVD GROWTH OF SI:H USING REAL TIME SPECTROSCOPIC ELLIPSOMETRY

D.H. Levi, B.P. Nelson, J.D. Perkins, and H.R. Moutinho
National Renewable Energy Laboratory, Golden, CO 80401

ABSTRACT

We have used in-situ real-time spectroscopic ellipsometry (RTSE) to characterize the morphology and crystallinity of hot-wire CVD (HWCVD) Si:H films as a function of hydrogen dilution R=[H]/[H+SiH_4], substrate temperature T_s, and film thickness d_b. Transitions from one mode of film growth to another are correlated with changes in the magnitude of the surface roughness during growth. The degree of crystallinity of the film can be determined from the form of the dielectric function. We have studied the growth parameter space for R from 0 to 14, T_s of 250°C and 500°C, and d_b from 0 to 1 um. We have mapped out the crystallinity vs. R, T_s, and d_b based on our analysis of the RTSE data. These results have been corroborated using Raman scattering and atomic force microscopy to characterize the crystallinity and surface morphology of the films.

INTRODUCTION

The properties of amorphous and microcrystalline hydrogenated silicon (a-Si:H and μc-Si:H) have attracted a great deal of research interest in recent years because of their application in thin-film solar cells and thin film transistors [1]. Of particular interest are the mechanisms occurring during film growth that are responsible for the transition from amorphous to microcrystalline growth. Improved understanding and enhanced control of these mechanisms will lead to higher-performance silicon thin-film devices.

Many studies have applied ex-situ measurement techniques to structural characterization of Si:H films, yet ex-situ approaches are limited in the information they can provide because μc-Si:H nucleation usually occurs at layer thicknesses below 500Å. In addition, the properties of μc-Si:H vary with film thickness. In-situ, real time spectroscopic ellipsometry (RTSE) provides an ideal characterization tool to study the amorphous to microcrystalline transition because it is able to monitor the evolution of the film thickness, surface roughness, and optical properties in real time during the film growth.

The utility of RTSE to study growth processes of thin-film a-Si:H and μc-Si:H has been demonstrated by Collins and co-workers in numerous studies [2]. Their studies have focused on plasma-enhanced CVD (PECVD) deposition of Si:H. They have established that the surface roughness of the growing film is a sensitive indicator of changes in the mode of film growth. An abrupt increase in surface roughness indicates a transition from stable a-Si:H growth to unstable a-Si:H growth, or from a-Si:H growth to a mixture of a-Si:H and μc-Si:H, or from mixed to purely μc-Si:H growth [3]. These transition points in the properties of the growing film have been expressed on a phase diagram by plotting the bulk thickness of the film where the transition occurs as a function of process variables such as dilution ratio R. These points can be linked to delineate regions of different growth modes as a function of deposition parameters.

EXPERIMENTAL DETAILS

All depositions were performed using a single 0.5 mm diameter W filament operated at a 60-Hz ac filament current of 16 amps (~2200°C). The filament is wrapped in a 4 mm diameter helix and mounted 4 cm from the substrates. The silane flow was fixed to 6 sccm with a silane partial pressure of ~3 mTorr. The two main deposition parameters varied in this study were the starting T_s, at either 250 or 500°C, and R from 0 to 14. All films were grown to a thickness of approximately 1 um. These experiments were carried out in the same chamber described in detail in [4] and under similar conditions to those in [5].

RTSE measurements were performed using a J.A. Woollam, Inc. M2000 visible and near IR rotating compensator ellipsometer and Woollam software for instrument control and data acquisition and analysis. The ellipsometer utilizes array detectors to collect spectra from 250 to 1700 nm, with an acquisition time as short as 100 ms. For this study spectra were collected from 255 to 1240 nm with an integration time of 200 to 500 ms during the nucleation phase of growth and 1 to 5 seconds during the later stages of growth, dependent upon film deposition rates. The angle of incidence was fixed at 70°.

The Raman scattering measurements were performed in a 180-degree backscattering configuration with a doubled Nd:YAG operating at 532 nm and a single grating Spex 270M spectrometer with a LN2 cooled CCD array detector. The incident laser power was 30 mW and a holographic notch filter was used to suppress the laser line. Penetration depth was approximately 96 nm for μc-Si:H and 64 nm for a-Si:H.

AFM measurements were performed using a Digital Instruments Dimension 3100 AFM, operating in tapping mode, using Si tips. RMS roughness values were calculated using the z-position of every pixel in the image.

Analysis of RTSE Data

RTSE data were analyzed in two stages. The early-time nucleation phase was modeled using a two-layer model, consisting of a bulk film with thickness d_b and a surface roughness layer with thickness d_s, both on top of a crystalline silicon substrate with a 15 Å thick native oxide layer. Most of the growth conditions required a third layer to represent a secondary phase of Si:H which started growing shortly after the nucleation phase had coalesced. The surface roughness layer was modeled using a Bruggeman effective medium approximation (EMA) of 50% void and 50% of the underlying material. The dielectric functions of the nucleation and post-nucleation layers were determined using an iterative optimization method to minimize the overall mean squared error within a selected region of growth time. Amorphous Si:H was modeled using a Cody-Lorentz oscillator formalism, while microcrystalline Si:H was modeled using a two-oscillator Tauc-Lorentz formalism [6].

In most of the films studied the optical properties of the film evolved during deposition. Multi-layer models do not work well to analyze the data as the film grows because of grading in the optical properties. In order to analyze the data after the initial nucleation phase, we have utilized a virtual interface (VI) model. The VI model cannot be applied during nucleation because it assumes a slowly varying surface roughness. The VI model fits the data using a 3-layer model consisting of 1) a surface roughness layer on top of 2) a growing film of thickness $5rt_o$, where r is the growth rate and t_o is the data acquisition interval, and 3) a pseudo-substrate with a pseudo-dielectric function $\langle\varepsilon\rangle$ calculated by directly inverting the psi and delta data at time t_{n-5}. The growing film of thickness $5rt_o$ is modeled as a 2-component Bruggeman EMA composed of a mixture of materials determined from the post-nucleation layer and the final material deposited at the end of the deposition. The growth rate r is held constant while the EMA percentage and surface roughness thickness are fit using regression analysis. In general, for each film three distinct dielectric functions are determined corresponding to the nucleation layer, the mid-layer, and the final layer. In the more homogeneous films some or all of these layers may be the same.

EVOLUTION OF SURFACE ROUGHNESS WITH FILM GROWTH

As discussed above, changes in the surface roughness are indications of changes in the growth mode of the film. A universal pattern for all films in this study is the initial nucleation and coalescence sequence. Figure 1 shows the evolution of d_s with time. There is a rapid initial increase in d_s as film growth begins at isolated nucleation sites, followed by a rapid decrease in d_s as the nucleation sites coalesce to form a continuous film. The amplitude of the initial peak in d_s is inversely correlated with the density of nucleation sites. Differences in the early time evolution of d_s are correlated with differences in the nucleation process of the film.

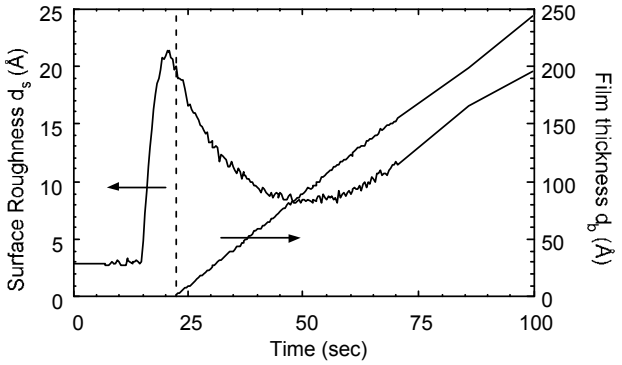

Figure 1. Evolution of d_s and d_b during nucleation and coalescence for the R=3, T_s=500°C sample. The dashed line indicates the coalescence of nucleation centers.

Figure 2 presents the evolution of d_s with d_b for the films grown at T_s=500°C. The behavior of d_s during the first few hundred angstroms, corresponding to the nucleation and initial stages of growth, is essentially the same for all films except for R=14. We conclude that the nucleation density is relatively constant for all films with R≤10 at T_s=500°C. Analysis of the dielectric functions of the nucleation layers in these films indicates that all films with R≤10 nucleate as a-Si:H, while R=14 nucleates as μc-Si:H. This is consistent with the relatively large values of d_s that the R=14 sample exhibits throughout growth. The evolution of d_s for d_b>300 Å indicates differences in films with different levels of dilution. The R=0 and R=3 films display almost identical behavior. Analysis of dielectric functions, as well as Raman scattering, show that both films are completely amorphous. Raman and RTSE data show that the R=4 and R=6 films are mixed-phase a-Si:H and μc-Si:H. The exceptionally large final values of d_s measured in these films have been corroborated by AFM measurements. AFM also shows these films have a distinct morphology, similar to grains of rice. The R=10 film is shown by Raman and RTSE to be primarily μc-Si:H, although it nucleates as a-Si:H. The R=14 film is μc-Si:H throughout its growth.

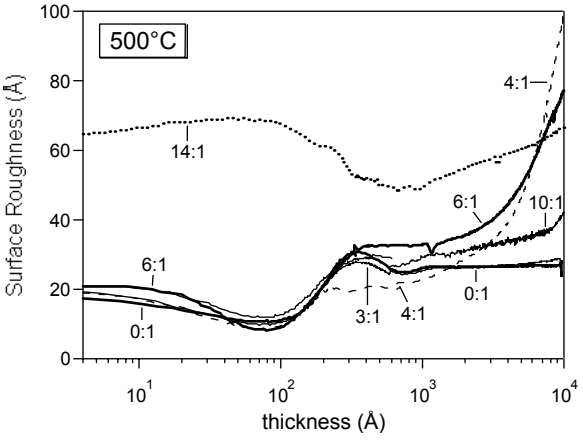

Figure 2. Evolution of d_s with d_b for T_s=500°C.

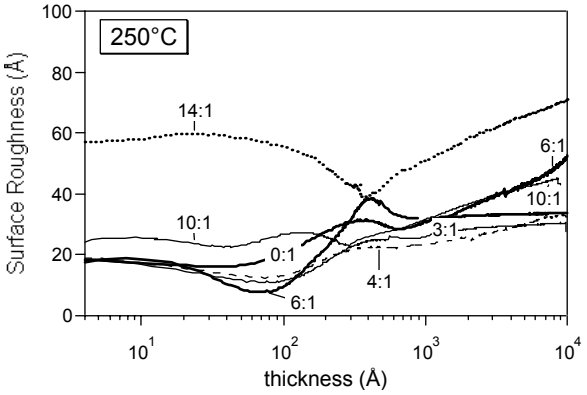

Figure 3. Evolution of d_s with d_b for T_s=250°C.

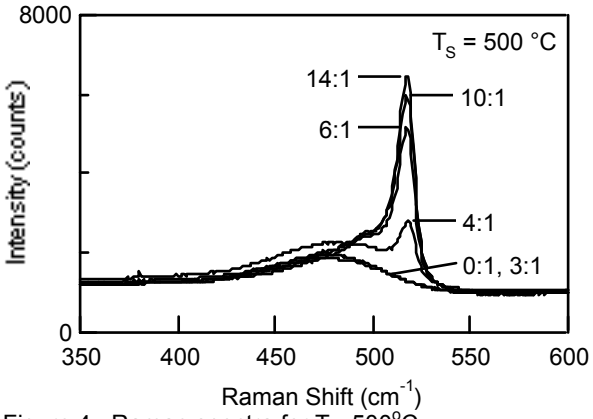

Figure 4. Raman spectra for T_s=500°C.

Figure 3 shows $d_s(d_b)$ data for the T_s=250°C films. The general trends for d_b<300 Å are similar to the T_s=500°C films with exceptions for R=0 and R=10. The R=0 film exhibits the same initial d_s as the other low-dilution films, but does not have the same degree of surface smoothening upon coalescence. We hypothesize this is because of reduced surface mobility of the deposition species due to the lower substrate temperature. The R=10 film exhibits a larger initial d_s. Analysis of the dielectric function of the nucleation layer in this film shows it to be transition or "edge" material, consistent with slightly greater initial surface roughness. The nucleation and coalescence behavior of the R=14 film are very similar to its T_s=500°C counterpart. For d_b>300 Å there is more scatter in the d_s behavior of the T_s=250°C films compared to the T_s=500°C films. Analysis of the dielectric functions as well as Raman scattering indicate that the onset of microcrystallinity occurs slighter earlier vs. dilution for the higher temperature growth conditions. The T_s=250°C films are also grown under more non-equilibrium type conditions as significant sample heating occurs during growth due to proximity to the 2200°C filament. This could account for more variations in the lower temperature films.

ANALYSIS OF CRYSTALLINITY

The degree of crystallinity of the films in this study was analyzed using in-situ RTSE and ex-situ Raman scattering. Raman scattering provides a semi-quantitative measure of crystallinity through the relative amplitudes of the amorphous and microcrystalline Raman peaks. Ellipsometry provides information on the degree of crystallinity from the dielectric function derived through analysis of the RTSE data. While Raman provides an average weighted by the intensity of the laser vs. depth, RTSE is able to provide a qualitative map of the crystallinity vs. depth in the film.

Figure 4 presents Raman scattering spectra for the T_s=500°C films. The broad peak at ~460 cm^{-1} is correlated with amorphous, while the sharp peak at ~530 cm^{-1} is correlated with microcrystalline silicon [7]. Penetration depths calculated at the 532 nm laser wavelength are 96 nm for microcrystalline and 64 nm for amorphous silicon. Because the degree of crystallinity varies with depth in the film, it is difficult to calculate an accurate ratio of amorphous to microcrystalline material based on the Raman scattering peak heights. The Raman data does provide a qualitative measure of the relative degree of crystallinity within the top 0.1 μm of these 1.0 μm thick samples. In addition, the Raman intensity scales with the degree of crystallinity, with small-grained μc-Si:H having a lower Raman intensity than large-grained μc-Si:H, and crystalline Si having a much higher intensity than any of the μc-Si:H samples measured in this study. We attribute this to final-state lifetime effects on the Raman scattering cross-section. Thus, the amplitude of the 530 cm^{-1} peak in the Raman spectrum is an indication of the degree of crystallinity of the μc-Si:H films.

It is clear in figure 4 that the R=0 and R=3 films are purely a-Si:H, whereas the R=4 film has a slight degree of crystallinity. The R=6,10, and 14 films are all predominantly μc-Si:H, with varying peak heights. This likely correlates with grain size in these μc-Si:H films. The trends for the T_s=250°C films are very similar to those noted for the T_s=500°C films. The R=4 film at T_s=250°C has somewhat less crystallinity than its T_s=500°C counterpart. Also, the R=6,10, and 14 films at T_s=250°C have a larger spacing in Raman intensity than their T_s=500°C counterparts, indicating larger difference in grain sizes for the μc-Si:H films grown at T_s=250°C.

Figure 5 is a representation of the degree of crystallinity versus depth based on evaluation of the dielectric functions derived from the RTSE data. As Si:H evolves from a-Si:H to μc-Si:H, both the amplitude and the peak energy of ε_1 and ε_2 increase. The amplitudes of ε_1 and ε_2 are also influenced by the presence of voids within the material. Because of this ambiguity in tracking crystallinity using the amplitude of the dielectric function, we have focused on the peak energies for ε_1 and ε_2. We have found that the peak in ε_1 evolves from 2.5 to 3.15 eV and the peak in ε_2 evolves from 3.6 to 4.15 eV as the film evolves from a-Si:H to μc-Si:H. Hence, in figure 5 the gray scale ranges from a sum of 2.5+3.6=6.1 eV to 3.15+4.15=7.3 eV, with white = 6.1 eV and black = 7.3 eV. White corresponds to completely amorphous and black

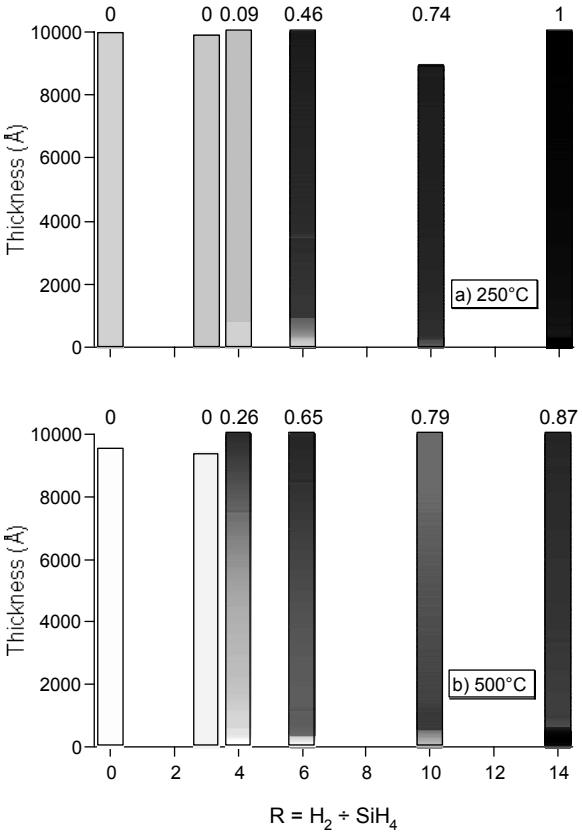

Figure 5. Grey scale plots of the evolution of the sum of ε_1 and ε_2 peak energies with thickness. Scale is from 6.1 eV (white, a-Si:H) to 7.3eV (black, μc-Si:H). Numbers across the top are the ratio of the 530 cm^{-1} Raman peak to highest measured in this study (≠ crystalline fraction).

corresponds to completely microcrystalline. Shades of gray represent varying degrees of crystallinity.

As described in the section on analysis, most films required three distinct dielectric functions for analysis of the in-situ RTSE data. This consisted of one function for the nucleation phase, one for the intermediate phase, and one for the end phase. Nucleation was described as a single or double layer, with the nucleation layer thickness allowed to vary as needed to fit the RTSE data. The remainder of the film was modeled as an EMA mixture of the intermediate and final dielectric functions. Thus the EMA % value provides a continuous scale between the intermediate and final endpoints. While this is admittedly a phenomenological, semi-quantitative approach to describing the crystallinity versus thickness, we believe that the results accurately describe how the relative degree of crystallinity evolves with substrate temperature, hydrogen dilution, and film thickness.

Figure 5(a) presents the evolution of crystallinity with thickness and hydrogen dilution for Ts=250°C. The numbers across the top give the ratio of the amplitude of the 530 cm^{-1} peak in the Raman spectrum to the highest intensity 530 cm^{-1} peak measured in this study. This number is roughly interpreted as the relative degree of crystallinity within the uppermost 1000Å of the film.

The homogeneous light gray shading for the R=0 and R=3 films in Figure 5(a) show that the R=0 and R=3 films are completely amorphous. This is confirmed by the Raman results. The R=4 film appears to be completely amorphous in the RTSE data, yet Raman indicates a small component of microcrystalline material at the surface. The R=6 film nucleates as a-Si:H, and grows primarily as μc-Si:H. The R=10 film nucleates as a material that appears to be midway between a-SiH and μc-Si:H, while the bulk of its growth is microcrystalline. Finally, the R=14 film is μc-Si:H at nucleation and throughout its growth.

Trends are very similar for the T_s=500°C films shown in figure 5(b). The R=0 and R=3 films are completely amorphous. Although the R=4 film nucleates as a-Si:H, it has a significantly greater μc-Si:H component than the T_s=250°C R=4 film. This is confirmed by the Raman results. The R=6 and R=10 films both nucleate as a-Si:H. although the R=10 nucleation layer has some microcrystalline character. An anomaly noted with the R=10 film is that it appears to become less crystalline as the film grows. We currently do not have an explanation for this behavior. The R=14 film nucleates and grows as μc-Si:H, as did the T_s=250°C R=14 film.

DISCUSSION AND CONCLUSIONS

RTSE measurements, as corroborated by Raman scattering and AFM, show that the transition from a-Si:H growth to μc-Si:H growth in HWCVD deposition of Si:H is relatively abrupt as a function of hydrogen dilution, whereas the transition occurs gradually as a function of film thickness.

ACKNOWLEDGMENTS

We acknowledge Rob Collins for many useful discussions and collaborations. This work was performed under DOE contract number DE-AC36-99GO10337.

1. Thin Solid Films, Vol. **395**, *Proceedings of the First International Conference on Cat-CVD (Hot-Wire CVD) Process*, edited by J.P. Conde, H. Masumura, and A.H. Mahan (Elsevier Science B.V., The Netherlands, June 2001)
2. R.W. Collins, Joohyun Koh, H. Fujiwara, P.I. Rovira, A.S. Ferlauto, J.A. Zapien, C.R. Wronski, R. Messier, *Appl. Surf. Sci.*, **154-155**, 217-228 (2000)
3. A.S. Ferlauto, R.J. Koval, C.R. Wronski, R.W. Collins, Mat. Res. Soc. Symp. Proc., Vol. **664**, A5.4 (2002)
4. B P. Nelson, et al, MRS Conference Proceedings, San Francisco, CA, April, 2002, A17.3, In Press.
5. D.H. Levi, et al, MRS Conference Proceedings, San Francisco, CA, April, 2002, A25.2, In Press.
6. A.S. Ferlauto, G.M. Ferreira, Chi Chen, P.I. Rovira, C.R. Wronski, R.W. Collins, X. Deng, G. Ganguly, "Optical metrology for the next generation of a-Si:H-based thin film photovoltaics," *Photovoltaics for the 21st Century II*, ed R.D. McConnell and V.K. Kapur (The Electrochemical Society, 2001) pp.199-228
7. Guozhen Yue, J. D. Lorentzen, Jing Lin, Qi Wang and Daxing Han, *APL.* **75**, 492 (1999).

REPORT DOCUMENTATION PAGE

Form Approved
OMB NO. 0704-0188

1. AGENCY USE ONLY (Leave blank)	2. REPORT DATE	3. REPORT TYPE AND DATES COVERED
	May 2002	29th IEEE PVSC-Conference Paper May 20-24 2002

4. TITLE AND SUBTITLE
In-situ Characterization of the Amorphous to Microcrystalline Transition in Hot-Wire CVD Growth of Si:H Using Real Time Spectroscopic Ellipsometry; Preprint

5. FUNDING NUMBERS
PVP21702

6. AUTHOR(S)
D.H. Levi, B.P. Nelson, J.D. Perkins, and H.R. Moutinho

7. PERFORMING ORGANIZATION NAME(S) AND ADDRESS(ES)
National Renewable Energy Laboratory
1617 Cole Blvd.
Golden, CO 80401-3393

8. PERFORMING ORGANIZATION REPORT NUMBER

9. SPONSORING/MONITORING AGENCY NAME(S) AND ADDRESS(ES)
National Renewable Energy Laboratory
1617 Cole Blvd.
Golden, CO 80401-3393

10. SPONSORING/MONITORING AGENCY REPORT NUMBER
NREL/CP-520-32283

11. SUPPLEMENTARY NOTES

12a. DISTRIBUTION/AVAILABILITY STATEMENT
National Technical Information Service
U.S. Department of Commerce
5285 Port Royal Road
Springfield, VA 22161

12b. DISTRIBUTION CODE

13. ABSTRACT *(Maximum 200 words):* This conference paper provides a brief look at the current U.S. research and development (R&D) investments in photovoltaics, covering the spectrum from materials and devices through electronics and systems reliability. The program is balanced among fundamental R&D, technology development, and systems performance and reliability, with more than half the funding for university and industry partners. The major activities can be categorized into two general areas: improving current and near-term technologies toward their expected performance levels (the largest portion), and positioning the United States for technical leadership, decision making, and ownership for the host of next-technology options (including some options that have been called third-generation). The investments in these higher risk, longer-term technology generations provide options that could leapfrog into more rapid use because of their promise of potentially high payoff. Solar electricity is part of America's present and future energy security and independence—as is the R&D that enables it.

14. SUBJECT TERMS: PV; research and development (R&D); technology development; systems performance and reliability; fundamental materials and device

15. NUMBER OF PAGES

16. PRICE CODE

17. SECURITY CLASSIFICATION OF REPORT	18. SECURITY CLASSIFICATION OF THIS PAGE	19. SECURITY CLASSIFICATION OF ABSTRACT	20. LIMITATION OF ABSTRACT
Unclassified	Unclassified	Unclassified	UL